



HIGH RESOLUTION X-RAY TOMOGRAPHY AS A TOOL FOR ANALYSIS OF INTERNAL TEXTURES IN METEORITES

Agata KRZESIŃSKA¹

¹ Polish Academy of Sciences, Institute of Geological Sciences, ul. Podwale 75, 50-449 Wrocław, Poland.

Abstract: A comparison of internal textures of the NWA-5929, Ghubara and Pułtusk chondrites has been carried out using high resolution X-ray tomography. This is a powerful, non-destructive technique that allows one to determine textural and compositional differences that occur between ordinary chondrites of various groups by means of grey-level scale histograms, first-order statistics, and 3D imaging.

Deformational structures in the Pułtusk meteorite such as cataclastic zones, impact melt clasts, melt veins, and melt pockets are observed and studied. Measurements of metal particle size are achieved, giving even deeper insight into textural features of meteorite. My approach shows that as shock deformation occurred, numerous small metal grains became progressively dispersed within the volume of the deformed Pułtusk meteorite rock. Simultaneously, metal was mobilized via frictional or direct impact melting to form scarce large metal nodules or grains arranged along the margins of relict chondritic clasts or as components of irregular injection veining.

The possibility of tracing of these impact related processes by using tomography micrograms (without breaking the sample) is very useful for distinguishing which parts of each meteorite were deformed in different ways in order to make first-order observations regarding the deformational history of these meteorites.

Keywords: NWA-5929, Ghubara, Pułtusk, high resolution X-ray computed tomography, deformation

INTRODUCTION

High resolution X-ray tomography (HR XCT) is a non-destructive method of analyzing solid-state bodies. For this reason, it has recently become one of the important tools for studying extraterrestrial materials like meteorites (Rubin et al., 2001; Ebel et al., 2008; Hezel et al., 2010; Kuebler et al., 1999; Nettles & McSween, 2006; Tsuchiyama et al., 2002), Antarctic micrometeorites (Okazawa et al., 2002), interplanetary dust particles, and material from sample-return missions (Nakamura et al., 2008). HR XCT was first utilized by Masuda et al. (1986) to study Antarctic meteorites in which silicates, sulphides and metal particles were distinguished, although no textural information was obtained because attainable resolution was then insufficient (~0.25 mm). The first real textural observations were carried out by Kondo et al. (1997), when they resolved porphyritic chondrules composed of euhedral crystals and surrounded by Fe-rich rims.

At that time, however, few works were dedicated to studying the internal textures of meteorites (Rubin et al., 2001; Žbik & Self, 2005) or the potential that HR XCT had for refining the classification of meteorites (Friedrich, 2008).

Textures of meteorites are still usually studied by making thin sections. This necessitates cutting the meteorite to be studied. However, with help of HR XCT, significant data on meteorites' internal texture may be collected without (or before) the partitioning of the sample. This paper shows that, with the aid of HR XCT, it is possible to demonstrate numerous differences between undeformed samples and samples that were cataclased or impact-melted with included metal veins or silicate-melt veins, melt pockets, and metal nodules. Author was also able to make semi-quantitative measurements of the volume of metal particles, allowing for inferences on the deformational processes involved.

Corresponding author: Agata KRZESIŃSKA, agatakrz@twarda.pan.pl

METHOD

The main parameter measured in high resolution X-ray tomography is a linear X-ray attenuation coefficient. In its simplest form, an X-ray fan beam in the tomographic instrument is directed at the object and the decrease in X-ray intensity caused by the passage through the object is measured by a linear array of detectors. The analysed object is rotated as measurements proceed, allowing it to be X-rayed at various orientations. At each rotation angle, the X-ray absorption is recorded and the obtained data are then reconstructed to create a cross-sectional image of the object along any arbitrary plane (Duliu, 1999; Uesugi et al., 2010). The difference of the X-ray absorption appears as the difference of computed tomography (CT) values in the image. A computer-aided generation of the resulting images relies on grey-scale variations within digital representations of the body being studied. The resulting picture is a stack of images of 8-bit 256-grey-scale colours. The grey-scales in such images reflect the relative linear X-ray attenuation coefficient, which is a function of density, atomic number and X-ray energy. When a mineral has larger X-ray absorption (higher X-ray attenuation coefficient) its CT value is larger and its image is brighter. Because the resulting values depend also on X-ray energy, calibration is needed for quantitative analyses.

SAMPLES USED IN EXPERIMENT

Samples of NWA-5929 (75 g) and Ghubara (9.5 g) as well as 23 samples of the Pułtusk meteorite (from 9.5 to 62 g) were analysed using HR XCT. They were analysed in their as-received states in the Institute of Gas and Oil, Kraków. A Benchtop CT160 high-resolution X-ray tomographic system was used in this study. The specimens were rotated 360° with X-ray projection images taken at 1° intervals. The X-ray source was operated at 160 kV. The voxel size (volumetric resolution) in tomography micrograms, determined by the 3D size of each sample, was 28.2 µm, 13 µm and 16.5 – 35.5 µm for the NWA-5929, Ghubara and Pułtusk samples, respectively.

The analyzed samples of Pułtusk meteorite were generously provided by the Museum of the Earth, Polish Academy of Sciences in Warsaw, Mineralogical Museum of the University of Wrocław, The Thugutt Mineralogical Museum on the Faculty of Geology, Warsaw University, Mineralogical Museum of Jagiellonian University in Kraków and the Geological Museum at the Institute of Geological Sciences PAS in Kraków.

Based on tomographic reconstructions, grey-level scale statistics were made and volume contents of metal were measured (Friedrich, 2008; Uesugi et al., 2010). In the next step, the HR XCT data were extracted for volumetric representations to obtain information about the shape of some elements and their relationship with their surroundings (Ketcham & Carlson, 2001; Ketcham, 2005; Carlson, 2006). Threshold tomograms were used in these reconstructions. ImageJ[®] was used as an open source program to manipulate image stacks and ImageJ 3D Viewer plugin was used for volumetric extractions.

Textural maturity descriptors of the analysed samples are based on grey-level co-occurrence matrices (GLCM) of the images (Petrou & Garcia Sevilla, 2006; Friedrich, 2008). The co-occurrence matrix represents the probability of the occurrence of a pair of grey values separated by a distance of 1 voxel at an angle $\Theta = 0^\circ$. Entropy and angular second moment quantify the degree of order within a GLCM. The inverse difference moment and contrast are parameters of the differences of grey-level scale values occurring within a GLCM. GLCM measurements for the analyzed samples are shown in table 1 and they reflect homogeneity of the samples which in turn relate to textural maturity (Petrou & Garcia Sevilla, 2006; Friedrich, 2008).

NWA-5929 meteorite is an unclassified chondrite composed of well preserved, large chondrules and euhedral grains of olivine and pyroxene. The chondritic matrix is fine grained, composed of silicates and a small fraction of metal-sulfide aggregates. Silicate grains are generally irregularly fractured.

Ghubara, an L-chondrite, was found in 1954 in Oman. It is a brecciated chondrite with several kinds of clasts differing in textures. They range from unequilibrated chondritic material to highly recrystallized, impact-melted and achondrite-like inclusions (Vinogradov and Vdovykin, 1963; Binns, 1967). The analyzed sample contains microcrystalline as well as porphyritic clasts (2–4 mm in size) of impact origin embedded in a highly deformed chondritic L5 host rock (Krzesińska & Siemiątkowski, 2011). The sample is veined and fractured.

The Pułtusk meteorite fell in 1868 in Poland. It is classified as H4-5 chondrite (Binns, 1967; Manecki, 1972) and its shock deformation stage is S3 (Stöffler et al., 1991). It is composed of H4 and H5 clasts. However, the cataclastic texture is overprinted on this

kind of brecciation (Krzyszewska, 2010a). Petrography of the samples used in the experiment has already been a subject of analyses. The results suggest that the meteorite experienced a complicated deformational history with impact melting and frictional melting acting during high strain-rate impacts on the parent body of the meteorite (Krzyszewska 2010a, b). Impact melt veins and clasts as well as metal veins and nodules are present in samples.

In this paper, the Pułtusk meteorite is studied more intensely than the others because of its much more complicated deformational history. Deformational structures analyzed by using HR XCT are shown with the obtained stack manipulation results. It clearly shows the usefulness of the HR XCT technique for solving some problems of deformational history reconstruction.

RESULTS

The different minerals present in meteorites appear on tomography micrograms as white, grey and dark colours which correspond to Fe-Ni alloy, troilite and silicates, respectively (Fig. 1). Silicate minerals such as olivine and pyroxene cannot be distinguished because difference in the X-ray absorption rate between them is too small. The same applies to kamacite and taenite.

The classification of meteorites is based on their chemical composition (chemical group) and their textural maturity acquired during the earliest metamorphism of a parent-body (Brearley & Jones, 1998; Van Schmus & Wood, 1967) as well as later impact deformation (Stöffler et al., 1991). Having taken into account that grey-level scale of tomograms in HR XCT reflects the volume content of the co-existing

Grey-level scale histogram

The sample of NWA 5929 contains a large fraction of chondrules with diameters up to 1 mm. They are particularly visible when encased by metallic rims. The measured metal content is 2.3% by volume. The dimensions of the metal grains (up to 0.5 mm) and their slightly irregular shapes are visible on the tomography micrograms (Fig. 1a). It is also seen that the meteorite contains significant amount of sulphides, though its abundance was not measured volumetrically.

The first-order statistics of the grey-level scale of the stacked images give the simplest textural descriptors. They are derived from the histogram of grey-level

Table 1. Grey-level statistics and 3D GLCM texture descriptors calculated for a GLCM created at distance 1 and with the angle 0. Values are in 256 color grey-level scale

	NWA 5929 LL	Ghubara L	Pułtusk H
metal volume content	2.3%	4.4%	7.1%
mean grey-level value	112	111	123
standard deviation	10.1	13.8	25
skewness	3.5	0.34	2.34
mode	108	110	107
minimum grey-level value	77	78	79
maximum grey-level value	226	225	255
GLCM			
Angular Second Moment	0.001	0.005	0.004
Contrast	268.553	205.472	354.799
Correlation	0.002	0.002	0.001
Inverse Difference Moment	0.199	0.304	0.137
Entropy	4.222	6.936	7.342

phases, the first-order statistics of the stacks of images were examined and described. These are the simplest textural descriptors derived from the generation of histogram of the grey-level scales contained within a digital dataset (for details see Petrou & Garcia Sevilla, 2006; Friedrich, 2008; Uesugi et al., 2010). The results obtained for NWA-5929, Ghubara, and Pułtusk are shown below.

On tomography micrograms, more discrete deformational structures were detected. It was possible to distinguish and precisely locate metal nodules, metal-free (achondritic-like) clasts in specimens, as well as melt pockets and silicate melt veins. By taking into account the reduced size and dispersion of Fe-Ni metal grains in some parts of the scanned specimens, it was possible to infer their cataclastic texture.

NWA 5929

scale (Fig. 1d). Values are presented in table 1. The mode value – the grey-level value that occurs most frequently (108) is related to silicates, the dominant phase of the sample. The mean value (112) is only slightly higher than the mode, which indicates that the fraction of other minerals in the sample is not significant. The standard deviation (10.1) shows, however, that there are many particles with significantly higher grey-level value than the mean. All of these parameters corroborate what was already known, that the meteorite is generally composed of silicates with small fractions of sulphides and metal.

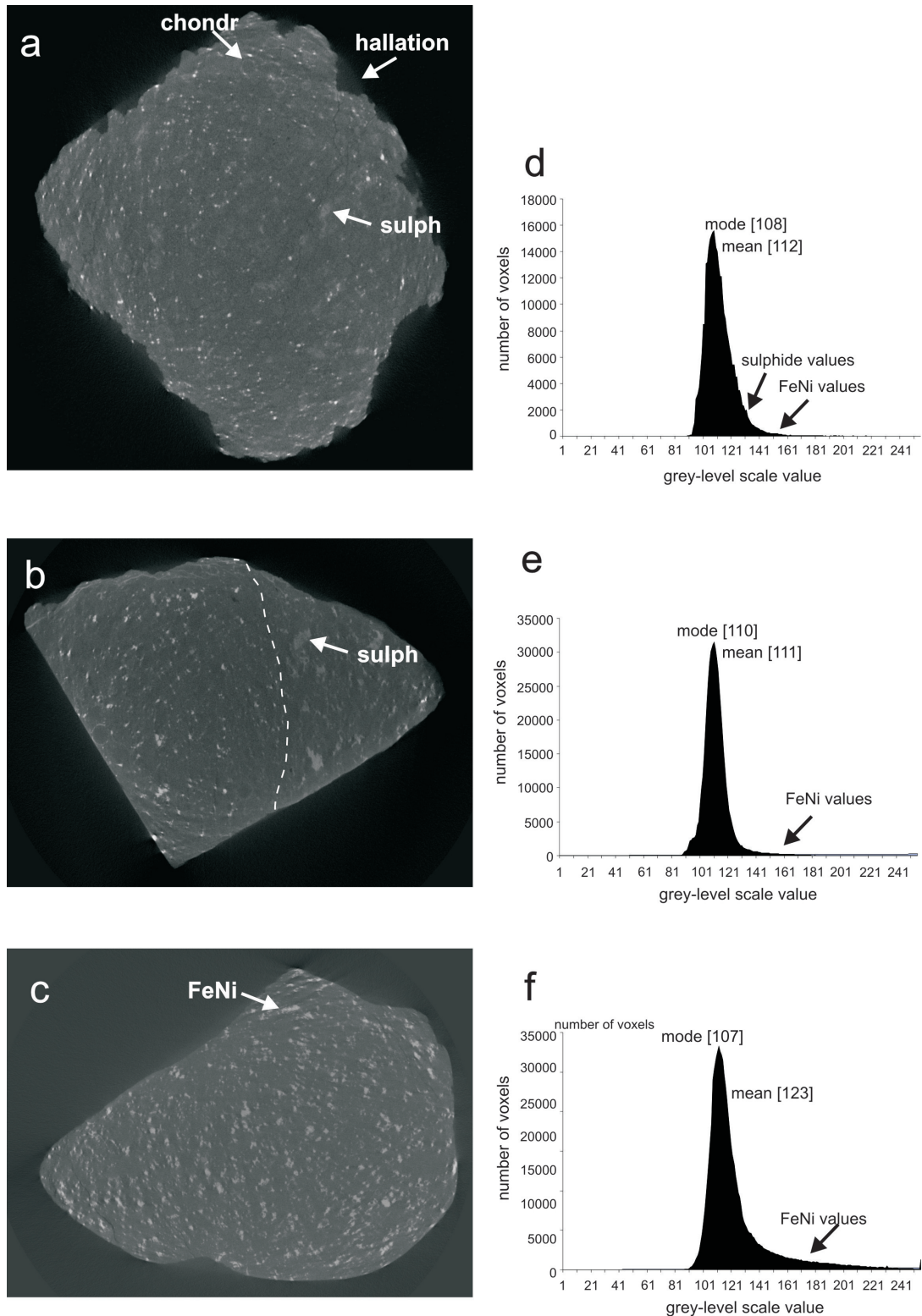


Fig. 1. Examples of tomography micrograms of the NWA-5929 (a), Ghubara (b) and Pultusk (c) meteorites. Tomography micrograms are constructed in 256- grey-level scale colours. Higher average atomic weight materials (metal) are brighter in the image. Background of an image is the darkest area as the air which surrounds chondrite is characterized by the least X-ray attenuation. Silicates are dark grey, sulphides are medium grey. Histograms of grey-level scale values for NWA-5929 (d), Ghubara (e), Pultusk (f) meteorites. The mode and mean values are pointed by arrows. Metal-values region is also shown and it is more represented in Pultusk than in NWA-5929 and Ghubara. chondr – chondrule; sulph – sulphide; FeNi – metal; hallation – an artifact due to irregular shape of the sample.

GLCM parameters show a low degree of order in the sample (angular second moment = 0.001 and en-

tropy = 4.222; Tab. 1) that suggests low textural maturity and metamorphic equilibration of the sample.

Ghubara

Grey-level scale histogram

The sample of Ghubara contains two different lithology types (Fig. 1b): one with abundant metal particles, and the other with many sulphides grains. Metal content by volume for the whole sample is 4.4%. The statistics of the grey-level scale is shown in table 1. The values are comparable with those obtained for NWA 5929, though the sulphide fraction is less represented

on the histogram (Fig 1e), indicated by the higher value of the standard deviation (13.8).

GLCM measurements show a high degree of order as the values of angular second moment and entropy are high (0.005, 6.936, respectively; Tab. 1). These suggest that the sample exhibits a higher degree of textural maturity. It is probably an equilibrated, high petrologic type.

Pułtusk

Grey-level scale histogram

Tomography micrograms of the Pułtusk meteorite show a large amount of metallic particles (Fig. 1c) and small fraction of sulphides. Sulphides generally form rare larger grains or nodules. The measured metal volume content amounts to 7.1%.

A large volume of metal is also seen in the grey-level scale histogram (Fig. 1f) and in the first-order statistics. The mean value of 123 is significantly higher than the mode value, ~107. This parameter and the high standard deviation (25) suggest large fraction of metallic particles.

GLCM descriptors show the homogeneous nature of the studied samples and point to their equilibration (Tab. 1). It was not possible to distinguish between H4 and H5 type material although clasts of the two types are present in the Pułtusk meteorite (Binns, 1967; Manecki, 1972).

Metal nodules and veins

In the analyzed samples, metal nodules and veins occur abundantly yet the volumetric metal content does not differ significantly between samples (Tab. 2). A visualization of the metallic bodies allowed for the determination of their shapes and spatial arrangements and further permitted inferences on their relationships with adjacent silicates. Examples of extracted metal nodules and veins are shown in figure 2.

Generally, nodules that occur in Pułtusk have irregular shapes and display two different textures: massive (Fig. 2a and 2b) and spongy (Fig. 2c). Although cross-sections through the massive nodules are elliptical, they are actually not ellipsoidal in 3D. An example of their interface with silicates is shown in figure 2b. Massive nodules are flattened and pinned by silicates, but the silicates are never embedded in the metal. In contrast, spongy nodules are characterized by the presence of many anhedral silicate grains dispersed in metal (Fig. 2c). The spongy nodule closely examined forms many injections into the surrounding silicate matrix, effectively blurring the boundary between

silicates and metal. In figure 2c, the nodule is located close to the fusion crust, however it penetrates deeply into the meteorite, with no relation to surface melting due to the stone's passage through the atmosphere.

Metal veins are also common in Pułtusk. They usually form planar sheets that continue sometimes as silicate-melt veins. Sets of parallel veins are visible in some specimens (Fig. 2d). Visualization of the metallic veins (Fig. 2e) allows obtaining information about their shape. The vein shown on figure 2d is displaced and bent due to dragging along the fault surface. Remobilization of metal into fractures must have occurred as prompted by the irregular shape of the vein. Such observations suggest that deformational processes operated in two stages: 1) emplacement of metallic veins and 2) displacements of plastically behaving veins and remobilization of melt forcibly injected into fractures.

Cataclastic zones

In general, cataclasis in chondrites is connected with the process known as darkening (Rubin, 1992; van der Bogert et al., 2003) which includes melting and dispersion of metal particles in the silicate matrix. Cataclastic portions of studied meteorites can be identified via the presence of small metal grains dispersed throughout the silicate matrix. Many samples of Pułtusk display darkening suggestive of cataclastic zones. In the cataclased domains, dimensions of metal particles were measured and they are shown in figure 3e and in table 2. Comparisons with the same measurements from undeformed samples demonstrate the presence of predominantly smaller grains near voxel size with a few larger metal nodules inside cataclastic domains.

Impact melt clasts and veins

Impact melt rock occurs only in one of the analysed samples, but many impact melt veins and melt pockets were detected in others samples. Because impact melt is composed of dispersed metal particles, the ma-

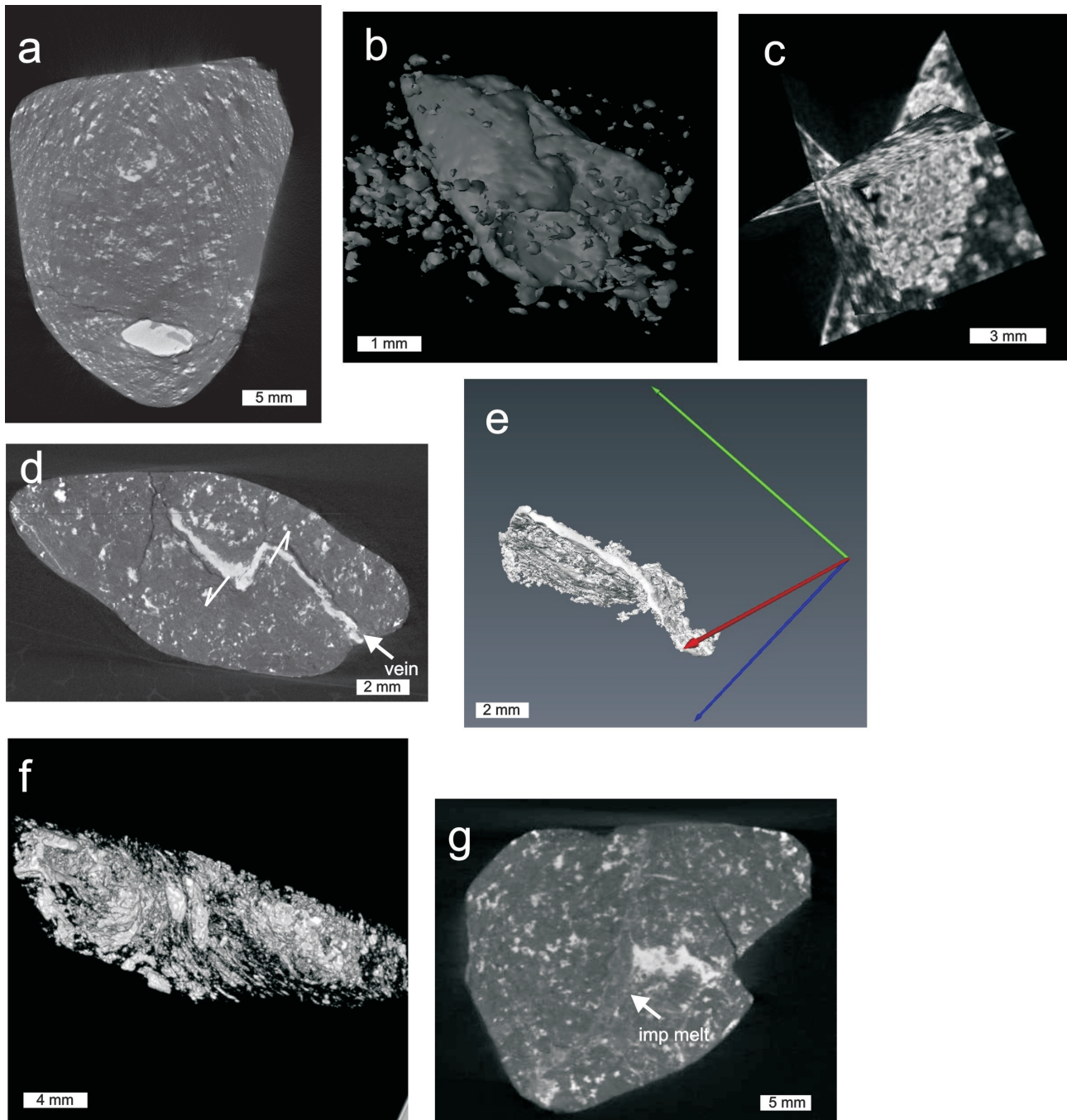


Fig. 2. Visualisation of deformational structures. The deformed bodies are extracted from the volumetric representation of Pułtusk samples; a – tomogram of the massive metal nodule; b – extracted nodule showing the contact with the matrix; c – spongy metal nodule with the silicates embedded into metal alloy; d – tomogram containing the metallic vein; e – extracted vein material showing its contact with the silicates and its geometry; f – extracted metal grains of impact-melt rock, flow-textured arrangement around chondritic relict clasts is pointed out; g – anastomosing impact melt veins in chondritic lithology and remobilized metal grains along the vein. Contrast is enhanced

jority of which are well below voxel size, the resulting grey-scale value is the mean for silicates and metals. Impact melt forms areas of light-grey colour on the tomography micrograms. By enhancing the contrast of the image, the presence of melt can be seen very distinctly. Figure 2g shows an example of an impact melt vein with anastomosed and embedded silicate clasts. Deformational evidence of the remobilization of metal grains along veins is also visible.

The most obvious textural evidence for impact melting is the flow-alignment of melted particles. This can be detected by sight, as shown in figure 2f. Large, elongated metal particles are arranged around clasts of unmelted and not deformed, chondritic material. Taking into account the mean grey-scale value of the phase between clasts, author inferred that the impact melt with metal surrounds chondritic clasts.

Progress of deformational processes – particle size histograms

In this study, volumetric analyses of all metal particles were performed in the not deformed, cataclased, and impact-melted samples of the Pułtusk meteorite. The results are shown in cumulative histograms in figures 3d-f and in table 2.

Dimensions of metal particles changed significantly as deformation and melting progressed. In the cataclased and impact-melted domains, the minimum size of the measured metal particles decreases to 1 voxel size ($20 \mu\text{m}$)³ and for not deformed samples the smallest metal particles are ~8 times the voxel size in diameter. Particles smaller than 1 voxel in diameter may be escaping our observation in the impact-melted regions because they are near the resolution limit for this technology. However, the volume of particles omitted from the analysis can not be large, because the whole sample volume metal content seems to not be affected.

In spite of the large fraction of small particles in cataclased and impact melted samples, some large metal grains appear. These metal grains are one order of magnitude larger than the largest ones in the undeformed sample. In the cataclased domains, the maximum measured value represents the size of a single anomalously large metal nodule. Within the impact melt, there are flow-arranged, elongated grains. The

Table 2. Measured metal particle size distribution in samples of Pułtusk meteorite. Values are in voxel size, what is ($20 \mu\text{m}$)³

	undeformed sample	cataclased sample	impact melt rock
minimum	8	1	1
maximum	126 482	2 473 500	2 676 656
median	85	64	22
mean value	916	714	467
metal volume content %	7.2%	7.1%	7.7%

number of large metal particles is, however, small. As can be seen in figures 3e and 3f, grains with a volume higher than 100 voxels make no more than 1% of the measured particles in the samples.

Although the biggest metal grains are much larger in the deformed samples than in the undeformed ones, the median value of metal particle size decreases with increasing deformation, whereas the half of the measured particles is smaller than the median. This has to be related to the large fraction of small metal particles in deformed samples. Because the median value decreases with increasing deformation, the number of small dispersed metal grains also increase with the degree of deformation. As the total volume of metal does not change in the analyzed samples, these testify melting and remobilization of metal alloy during deformational processes to voluminous, scarce metal grains and more and more dispersed small metal particles.

DISCUSSION

The presented results of high resolution X-ray tomography measurements show that the volume of metal particles differs distinctly between the Pułtusk, NWA-5929, and Ghubara chondrites (Tab. 1). Moreover, the sulphide phase is more abundant in NWA-5929 than in Pułtusk. This may reflect decrease in overall metal volume and an increase of sulphide phases from the H- to L-chondrites (Brearley and Jones, 1998). The measured metal content value for the NWA-5929 chondrite proves it is an LL/L chondrite.

The measured metal content for the Pułtusk meteorite samples used is 7.1–7.7 vol%. The metal content of Pułtusk was previously measured via HR XCT (Žbik and Self, 2005) and the achieved value 7.7 vol. % correlates well with the results of this study.

The data shown in histograms (Figs. 1d–f) and in the digital set reflect the differences in the content of silicates, sulphides and metal phases, yet point to overall similarities in mineral composition with silicates as the dominant phase. With the same minimum, maximum and mode values of intensity in grey-level scale (the all studied samples are composed of the same

minerals, mainly of silicates), the mean value apparently increases from the relative lowest in NWA-5929 and Ghubara to the highest in the Pułtusk chondrites (Tab. 1). It is shown that grey-level scale histograms and statistics estimated from image stacks reflect changes in the mineralogy of meteorites. However, it is important to keep in mind that the value of the grey scale depends not only on the phase composition but also on the X-ray energy. So, only semi-quantitative results are obtainable.

HR XCT technique can provide useful and significant information about the internal textures of meteorites. It provide us with a new and nondestructive means of assigning chondrites to their proper chemical groups as well as providing us with additional information on their metamorphic histories and textural maturity. However, comparison of the petrographic and microstructural analyses of Pułtusk (Krziesinska, 2010a, b) and Ghubara (Krziesinska & Siemiątkowski, 2011) meteorites clearly shows that one cannot reliably distinguish between petrologic types with this technique.

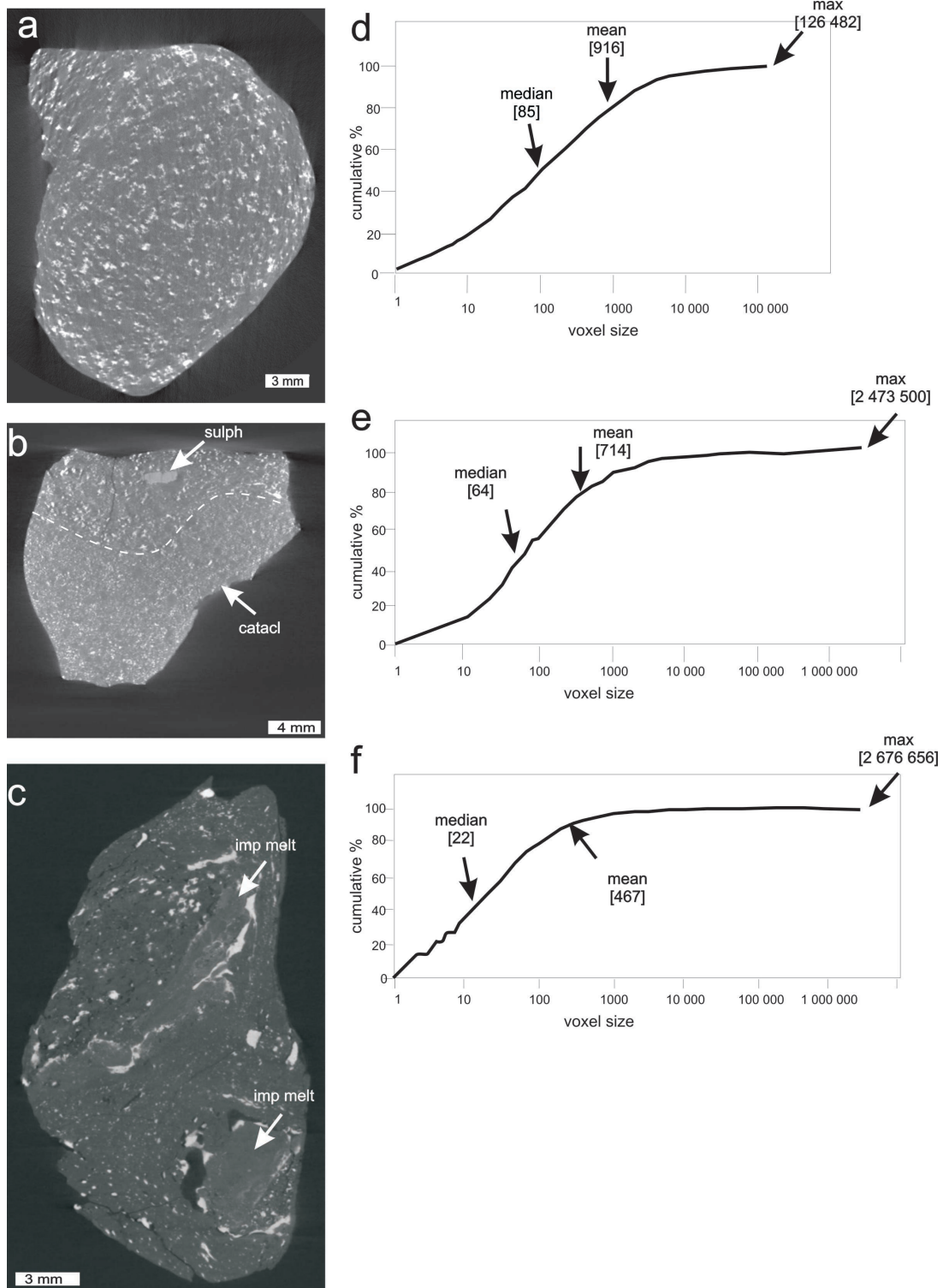


Fig. 3. Tomography micrograms of specimens of the Pułtusk meteorite. a – not deformed, b – cataclased, c – impact melted. Cumulative histograms of metal particle size in these samples: d – not deformed, e – cataclased, f – impact-melted. The size of particles is in voxel size ($20 \mu\text{m}^3$). The mean size decreases with the progress of deformation and melting and concurrent formation of large but scarce metallic particles. These large grains are metal nodules and flow-textured remobilized metal grains within the melted domains. Statistical values are shown on histograms and in table 2

Comparison of textural analyses of Pułtusk samples (Krzesińska, 2010b) with HR XCT results shows that using this technique it is possible to trace deformational processes like cataclasis, impact-melting, veining, and metallic melt remobilization. Moreover,

HR XCT technique enable us to identify the strong negative correlation between the degree of shock-induced deformation of chondritic meteorites with the size of the metal particles they contain.

CONCLUSIONS

In principle, HR XCT can be used to examine structures of any chondrite component which possesses an X-ray attenuation different from its surrounding material. It is a semi-quantitative tool useful for the chemical classification of chondrites.

By using HR XCT we can trace several processes such as cataclasis (Figs. 3b, 3e), impact melting (Figs. 2f, 3c, and 3f), fracturing (Fig. 2d), formation of melt pockets (Fig. 2g), and metal veins (Figs. 2d, 2e) and nodules (Figs. 2a–c). HR XCT also allows for the semi-quantitative characterization of the size and shape of metal particles (Figs. 3d–f) and voids, and further permits us to make suppositions about the spatial arrangement of deformed areas and, in some

cases, to draw conclusions about the sequence of deformational events.

This study is important because it shows that such information can be obtained without sample destruction, in their as-received state. The obtained images may furnish information about textural and compositional features of objects as small as few micrometers, depending on resolution. However, the technique is not without limitation, as the computed tomography can only be used for the study of small samples (up to ~70 g) of meteorites. Despite this limitation, HR XCT technique proves to be a powerful tool, particularly indispensable for studying the textural characteristics of meteorites, and it holds obvious advantages as a non-destructive method.

ACKNOWLEDGMENTS

This research was funded by the Ministry of Science and Higher Education of Poland as a part of the project N N307 474838. The analysed samples of the Pułtusk meteorite were generously provided by the Museum of the Earth, Polish Academy of Sciences in Warsaw, Mineralogical Museum of the University of Wrocław, The Thugutt Mineralogical Museum of the Faculty of Geology, Warsaw University, Mineralogical Museum of Jagiellonian University in Kraków and the Geological Museum at the Institute of Geological Sciences

PAS in Kraków. I would like to thank Dr. Tomasz Jakubowski for donating the sample of NWA 5929 chondrite for analysis. Mgr Marek Dohnalik and mgr Jan Kaczmarczyk are thanked for tomographic scanning of the samples. Prof. Andrzej Żelaźniewicz is acknowledged for improvement of the early version of the manuscript. Prof. Ryszard Kryza and Anonymous Reviewer are thanked for careful and helpful review and suggestions that improved the manuscript.

REFERENCES

- Binns R.A., 1967 – Cognate xenoliths in chondritic meteorites: examples in Mezo-Madras and Ghubara. *Geochimica et Cosmochimica Acta*, 32 (3), 299–317.
- Brearley A.J., Jones R.H., 1998 – Chondritic meteorites. [in:] Planetary Materials, Rev. in Min., 36 (ed. J.J. Papike), 3-1–3-398.
- Carlson W.D., 2006 – Three-dimensional imaging of earth and planetary materials. *Earth and Planetary Science Letters*, 249 (3-4), 133–147.
- Duliu O.G., 1999 – Computer axial tomography in geosciences: an overview. *Earth-Science Reviews*, 48 (4), 265–281.
- Ebel D.S., Weisberg M.K., Hertz J., Campbell A.J., 2008 – Shape, metal abundance, chemistry, and origin of chondrules in Renazzo (CR) chondrite. *Meteoritics & Planetary Science*, 43 (10), 1725–1740.
- Friedrich J.M., 2008 – Quantitative methods for three-dimensional comparison and petrographic description of chondrites. *Computers & Geosciences* 34 (12), 1926–1935.
- Hezel D.C., Needham A.W., Armytage R., Georg B., Abel R., Kurahashi E., Coles B.J., Rehkaemper M., Russell S.S., 2010 – A nebula setting as the origin for bulk chondrule Fe isotope variations in CV chondrites. *Earth and Planetary Science Letters*, 275 (1–2), 132–180.
- Ketcham R.A., 2005 – Three-dimensional grain fabric measurement using high-resolution X-ray computed tomography. *Journal of Structural Geology*, 27 (7), 1217–1228.
- Ketcham R.A., Carlson W.D., 2001 – Acquisition, optimization and interpretation of X-ray computed tomographic imagery: applications to the geosciences. *Computers & Geosciences*, 27 (4), 381–400.
- Kondo M., Tsuchiyama A., Hirai H., Koishikawa A., 1997 – High resolution X-ray computed tomographic (CT) images of chondrites and chondrules. *Antarctic Meteorite Research*, 10, 437–447.
- Krzesińska A., 2010a – Polyphase deformation of the Pułtusk meteorite. *Meteoryt*, 75 (3), 3–6 (in Polish).
- Krzesińska A., 2010b – Oblique impact-induced (shock-related) shearing and frictional melting in Pułtusk (H5) chondrite. 41st Lunar and Planetary Science Conference. Abstract #1140. CD-ROM.
- Krzesińska A., Siemiątkowski J., 2011 – Evidence for multiple deformational brecciation and impact melting in chondrites from the Jacek Siemiątkowski collection. *Przegląd Geologiczny*, 59 (8), 576–588 (in Polish with English summary).
- Kuebler K.E., McSween H.Y., Carlson W.D., Hirsch D., 1999 – Sizes and masses of chondrules and metal-troilite grains in

- ordinary chondrites: possible implications for nebular sorting. *Icarus*, 141 (1), 96–106.
- Maneck A., 1972 – Mineralogical-petrographic study of the Pułtusk meteorite. *Prace Mineralogiczne PAN*, 27, 53–69 (in Polish).
- Masuda A., Taguchi I., Tanaka K., 1986 – Non-destructive analysis of meteorites by using a high-energy X-ray scanner. Papers presented to the 11th Symposium on Antarctic Meteorites. March 25–27, 1986. Tokyo, Nat. Inst. Polar. Res., 148–149.
- Nakamura T., Noguchi T., Tsuchiyama A., Ushikubo T., Kita N., Valley J.W., Zolensky M.E., Kakazu Y., Sakamoto K., Mashio E., Uesugi K., Nakano T., 2008 – Chondrule like objects in short period comet 81P/Wild 2. *Science*, 321 (5896), 1664–1667.
- Nettles J.W., Mc Sween Jr. H.Y., 2006 – A comparison of metal-troilite grain size distribution for type 3 and type 4 ordinary chondrites using X-ray CT data. *Lunar and Planetary Sciences Conference XXXVII*, abstract #1996.
- Okazawa T., Tsuchiyama A., Yano H., Noguchi T., Osawa T., Nakano T., Uesugi K., 2002 – Measurement of densities of Antarctic micrometeorites using X-ray microtomography. *Antarctic Meteorites*, 9, 79–96.
- Petrou M., García Sevilla P., 2006 – Image Processing: dealing with Texture. Wiley, New York. 618.
- Rubin A.E., 1992 – A shock-metamorphic model for silicate darkening and compositionally variable plagioclase in CK and ordinary chondrites. *Geochimica et Cosmochimica Acta*, 56 (4), 1705–1714.
- Rubin A.E., Ulf-Møller F., Wasson J., Carlson W.D., 2001 – The Portales Valley meteorite breccia: Evidence for impact-induced melting and metamorphism of an ordinary chondrite. *Geochimica et Cosmochimica Acta*, 65 (2), 323–342.
- Tsuchiyama A., Nakamura T., Nakano T., Nakamura N., 2002 – Three-dimensional description of Kobe meteorite by micro X-ray CT method: possibility of three-dimensional curation of meteorite samples. *Geochemical Journal*, 36 (4), 369–390.
- Stöffler D., Keil K., Scott E.R.D., 1991 – Shock metamorphism of ordinary chondrites. *Geochimica et Cosmochimica Acta*, 55 (12), 3845–3867.
- Uesugi M., Uesugi K., Oka M., 2010 – Non-destructive observation of meteorite chips using quantitative analysis of optimized X-ray micro-computed tomography. *Earth and Planetary Science Letters*, 299 (3–4), 359–367.
- van der Bogert C.H., Schultz P.H., Spray J.G., 2003 – Impact-induced melting in ordinary chondrites: a mechanism for deformation, darkening, and vein formation. *Meteoritics & Planetary Science*, 38 (10), 1521–1531.
- Van Schmus W.R., Wood J.A., 1967 – A chemical-petrologic classification for the chondritic meteorites. *Geochimica et Cosmochimica Acta*, 31 (5), 747–765.
- Vinogradov A.P., Vdovykin G.P., 1963 – Diamonds in stony meteorites. *Geochemistry*, 8, 743–750.
- Żbik M., Self P., 2005 – High resolution X-ray microtomography analysis in non-destructive investigation of internal structure in two chondrites. *Mineralogia Polonica*, 36 (1), 5–19.